Infrared Spectroscopy of $[XFeC_{24}H_{12}]^+$ (X = C_5H_5, $C_5(CH_3)_5$) Complexes in the Gas Phase: Experimental and Computational Studies of Astrophysical Interest

Aude Simon* and Christine Joblin

Centre d'Étude Spatiale des Rayonnements, Université Toulouse III—CNRS, Observatoire Midi-Pyrénées, 9 Avenue du Colonel Roche, BP 44346, 31028 Toulouse Cedex 4, France

Nick Polfer† and Jos Oomens

FOM Institute for Plasma Physics "Rijnhuizen", Edisonbaan 14, NL-3439MN Nieuwegein, The Netherlands

Received: February 20, 2008; Revised Manuscript Received: June 17, 2008

We report the first experimental mid-infrared (700−1600 cm^{-1}) multiple-photon dissociation (IRMPD) spectra of $[XFeC_{24}H_{12}]^+$ (X = C_5H_5 or Cp, $C_5(CH_3)_5$ or Cp*) complexes in the gas phase obtained using the free electron laser for infrared experiments. The experimental results are complemented with theoretical infrared (IR) absorption spectra calculated with methods based on density functional theory. The isomers in which the XFe unit is coordinated to an outer ring of $C_{24}H_{12}^+$ (Out isomers) were calculated to be the most stable ones. From the comparison between the experimental and calculated spectra, we could derive that, (i) for $[CpFeC_{24}H_{12}]^+$ complexes, the ^{1}A Out isomer appears to be the best candidate to be formed in the experiment but the presence of the ^{1}A In higher energy isomer in minor abundance is also plausible; and (ii) for $[Cp^*FeC_{24}H_{12}]^+$ complexes, the three calculated Out isomers of similar energy are likely to be present simultaneously, in qualitative agreement with the observed dissociation patterns. This study also emphasizes the threshold effect in the IRMPD spectrum below which IR bands cannot be observed and evidence strong mode coupling effects in the $[XFeC_{24}H_{12}]^+$ species. The effect of the coordination of Fe in weakening the bands of $C_{24}H_{12}^+$ in the 1000−1600 cm^{-1} region is confirmed, which is of interest to search for such complexes in interstellar environments.

I. Introduction

Léger and Puget[1] and Allamandola et al.[2] suggested in the early 1980s that polycyclic aromatic hydrocarbons (PAHs) and PAH-related molecules are the major carriers of the discrete emission infrared (IR) spectrum that is observed ubiquitously in the interstellar medium (ISM) in the 3−13 μm (770−3100 cm^{-1}) range. Since then, many studies, laboratory experiments [3−14] and theoretical calculations, [15−25] have been dedicated to the identification of the carriers of these features, the so-called aromatic infrared bands (AIBs) at 3.3, 6.2, 7.7, 8.6, 11.3, and 12.7 μm (3030, 1613, 1299, 1663, 885, and 787 cm^{-1}). There is now compelling evidence that these features are due to a complex mixture of ionized and neutral, possibly substituted or complexed, PAHs of large sizes,[26−36] but no satisfactory match to the observed spectra has been obtained yet.

Serra et al.[37] and Chaudret et al.[38] suggested that interstellar PAHs could coordinate efficiently to metal atoms. In particular, the important depletion of metallic iron from the gas phase could partially be accounted for by its coordination to PAHs to form stable complexes. The authors also suggested a catalytic role of the coordinated iron in the growth of carbon macromolecules.[39] The proposal by Serra et al.[37] and Chaudret et al.[38] opened a new class of species to be considered. It motivated at the time a few experimental[40,41] and theoretical[42,43] studies on small iron−PAH systems, along with astrophysical modeling.[44]

Spectroscopic data on iron complexes containing large PAHs, as would be expected in interstellar space, are scarce. Simon and Joblin recently published a theoretical study which shows the general trends for the influence of iron coordination on the IR spectra of neutral and cationic PAHs.[45] The most affected region is the 1000−1600 cm^{-1} region, where the CH in-plane bending (δ_{CH}) and CC stretching (ν_{CC}) modes of PAHs are found. These bands are intense for bare cationic PAHs and weak for bare neutral PAHs. The coordination of Fe has a "moderating" effect, decreasing their intensities for cationic PAHs and increasing them for neutral PAHs, which finally leads to comparable spectra for both neutral and cationic FePAH complexes. Experimental IR spectra of neutral iron−pyrene and iron−coronene complexes in cold matrices were obtained by Elustando et al.[46] and Wang et al.[47] The observed features are reported to be in agreement with the calculated IR spectrum of the iron−coronene neutral complex in its triplet spin state, which was determined as the ground state.[47] Interestingly, recent calculations report a quintet spin state as the ground state of $FeC_{24}H_{12}$.[45] This illustrates the importance of combining experiments and calculations to improve our knowledge of these systems.

It is now accepted that emission in the AIBs arises from hot gas-phase PAH-like species following excitation by UV−visible photon absorption. Oomens et al. have shown that a good technique to mimic these spectra in the laboratory is to perform infrared multiple-photon dissociation (IRMPD) experiments, where ions are irradiated with the intense and tunable IR light of a free electron laser (FEL). The photodissociation yield as a function of the wavelength gives the IRMPD spectrum. Oomens

* To whom correspondence should be addressed.
† Present address: Department of Chemistry, University of Florida, P. O. Box 117200, Gainsville, FL 32611.

10.1021/jp801517q CCC: $40.75
Published on Web 08/26/2008

et al.[11,12] obtained the IRMPD spectra of cationic PAHs in a quadrupole ion trap at FELIX (free electron laser for infrared experiments)[48] and worked on their modeling.[12,49] More recently, the IRMPD spectra of FeY^+ and FeY_2^+ (Y = C_6H_6, $C_{10}H_8$, and $C_{13}H_{10}$) complexes trapped in the cell of a Fourier transform ion cyclotron resonance mass spectrometer (FTICRMS) were recorded at FELIX by Szczepanski et al.[50] IRMPD spectroscopy is also a dedicated experimental technique to obtain direct information on the geometric and electronic structures as well as on the spin states of small ionic complexes in the gas phase. The combination of IRMPD spectroscopy and density functional theory (DFT) calculations has allowed identification of structures in biomolecules[51−54] and organometallic complexes,[55] which have quite complicated ground-state potential energy surfaces.

As emphasized above, spectroscopic data for organometallic systems involving iron and large PAHs are scarce. This is in a way understandable since obtaining reliable data on large unsaturated organometallic π-complexes represents a challenge for both theory and experiments. $[FeC_{24}H_{12}]^+$ and $[Fe(C_{24}H_{12})_2]^+$ complexes were produced for the first time in an FTICR cell by the group of R. C. Dunbar[56] using radiative association of Fe^+ formed by laser ablation of a metallic target and $C_{24}H_{12}$ as a vapor. However, the low vapor pressure of coronene makes the use of this technique difficult for the production of the complex. Efforts have been dedicated to produce multimetal−multiligand iron−coronene complexes in the gas phase in the group of M. A. Duncan. A variety of cationic metal−PAH clusters were formed by covaporization of materials in a laser plasma source.[57] Mixtures of metal powder, metal oxides, or other materials with the PAH of interest were ablated with a pulsed Nd:YAG laser, but iron−PAH complexes happened to be particularly difficult to produce by this method. An efficient technique to form $[Fe_x(C_{24}H_{12})_y]^+$ complexes in the gas phase consists of using a pulsed nozzle laser vaporization cluster source with a metal rod coated with a sublimed film of coronene.[58] However, such a source has not been available yet at mass spectrometers interfaced with FELs. Another effort led by Simon and Joblin with the PIRENEA FTICR setup[59] consists of producing iron−PAH complexes by laser ablation of solid targets that are mixtures of PAHs and organometallic precursors. The advantage of this production mechanism is that it can be easily reproduced in other FTICR setups, in particular the one available at FELIX for IRMPD studies.

In this contribution, we present the experimental IRMPD spectra of $[XFeC_{24}H_{12}]^+$ (X = C_5H_5 or Cp, $C_5(CH_3)_5$ or Cp*) complexes (section III.B) and the calculated IR absorption spectra of their lowest energy isomers at the DFT level (section III.C). We then discuss (section III.D) how the comparison between experimental and theoretical results can bring insights into (i) the validity of the calculations and (ii) the properties of these large organometallic systems, in particular metal−ligand binding energies and vibrational mode couplings. Finally, the astrophysical implications of these results are given in section III.E.

II. Methods

A. Experimental Methods. The experiments were carried out at FELIX[48] using the home-built 4.7 T FTICR mass spectrometer.[60] The ions were formed by single-shot laser ablation of a solid target made of a 2:1 mixture of $[XFe(CO)_2]_2$ (X = C_5H_5 or Cp, $C_5(CH_3)_5$ or Cp*) and $C_{24}H_{12}$ purchased from Sigma-Aldrich. The 355 nm output of a Nd:YAG laser was used with attenuation (8.6 mJ/pulse) and defocusing. The ions were allowed to relax for 2 s in the ICR cell, and the species of interest ($[CpFeC_{24}H_{12}]^+$ or $[Cp^*FeC_{24}H_{12}]^+$) were isolated by ejection of all other ions using a stored-waveform inverse Fourier transform (SWIFT) pulse.[61,62] The mass-selected ions were irradiated for 10 s using the focused output of the FELIX laser, which delivers 5 μs long macropulses consisting of a train of approximately 1 ps long micropulses separated by 1 ns. The wavelength of FELIX can be tuned continuously between 3 and 250 μm. In this study, only the 6−14 μm (710−1670 cm^{-1}) range was used, which can be covered with one single setting of the electron beam energy (≈40 MeV). The wavelength was scanned in 0.02 μm steps. The width of FELIX is ∼0.5% of the wavenumber; thus, the full width at half-maximum (fwhm) is ∼4 cm^{-1} at 800 cm^{-1} and ∼8 cm^{-1} at 1600 cm^{-1}.

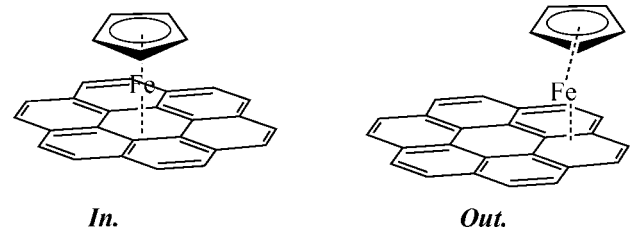

Figure 1. In and Out isomers of the $[CpFeC_{24}H_{12}]^+$ complexes.

It is now commonly accepted that, at a vibrational resonance, the irradiated species absorb multiple infrared photons in a noncoherent fashion. After absorption, intramolecular vibrational redistribution (IVR) randomizes the absorbed energy over the bath of vibrational states.[63,64] This process effectively heats the complex until the energy is sufficient for statistical dissociation to occur. The total fragmentation yield $P_{frag.}$, recorded as a function of wavelength, gives the IRMPD spectrum. $P_{frag.}$ can be expressed as

$$[P_{frag.}]\lambda = \left[\frac{\Sigma I_{fragments}}{\Sigma I_{fragments} + I_{parent}}\right]\lambda \qquad (1)$$

where $\Sigma I_{fragments}$ is the sum of the abundances of the photofragments and I_{parent} the abundance of the parent ion.

Only the $CpFe^+$ photofragment is observed for $[CpFeC_{24}H_{12}]^+$, whereas several photofragments ($C_{24}H_{12}^+$, $C_{24}H_{13}]^+$, $[FeC_{24}H_{13}]^+$, $[FeC_{10}H_{13}]^+$, and $[FeC_{10}H_{15}]^+$) are observed for $[Cp^*FeC_{24}H_{12}]^+$, revealing a complex fragmentation chemistry involving hydrogen transfers from the Cp* ligand. The dissociation features of $[XFeC_{24}H_{12}]^+$ (X = Cp, Cp*) complexes under continuous UV−visible irradiation and sustained off-resonance irradiation collision-induced dissociation (SORI-CID)[65,66] conditions were studied in the PIRENEA setup[59] prior to the IRMPD experiments at FELIX. The results are presented and discussed in section III.A.

B. Computational Method. DFT calculations were performed to determine the most stable structures for the $[CpFeC_{24}H_{12}]^+$ and $[Cp^*FeC_{24}H_{12}]^+$ complexes and obtain their IR absorption spectra. Geometry optimizations and harmonic frequency calculations were performed at the B3LYP[67]/Lanl2DZ[68] level of theory. The hybrid Hartree−Fock/DFT functional B3LYP was chosen for the first systematic study of the IR spectra of a series of neutral, cationic, and anionic PAHs ranging from naphthalene to ovalene,[19] leading to good agreement with the available experimental spectra, and has now been used to establish a spectroscopic database for PAHs.[25] The calculations were performed using the Gaussian03 software.[69] Only structures with metal−ligand π-interactions were considered as they are expected to be the most stable ones. The two types of investigated structures are shown in Figure 1. The structure with the XFe^+ unit interacting with the inner ring of

coronene is designated as the "In" isomer. When the XFe^+ unit coordinates to an outer ring, it is designated as the "Out" isomer. For each structure, the three possible spin multiplicities $2S + 1 = 5$, 3, and 1 were considered. Formally, the $FeCp^+$ unit has the same number of d electrons as the iron atom for which the ground state is a quintet spin state (^{5}D); the first triplet and singlet spin- states (^{3}F and ^{1}G, respectively) lie respectively 1.48 and 3.05 eV higher.[70] Ab initio studies by Sodupe and Bauschlicher[71] also showed that the ground state for $FeCp^+$ is a $^5A_2$ state. The theoretical determination of the electronic and vibrational structures for large organometallic systems such as $[XFeC_{24}H_{12}]^+$ (X = Cp, Cp*) is difficult since the best alternative is the use of DFT methods with small basis sets, and these methods often lack experimental verification. The thermochemical and spectroscopic results obtained for model FePAH and $FePAH^+$ complexes at the B3LYP/Lanl2DZ level have been previously compared to those obtained at the MPW1PW91[72,73]/6-31+G(d,p) level.[45] Similar electronic structures were obtained for the ground states at the two levels of theory as well as very similar IR spectra in the 3−20 μm (500−3300 cm^{-1}) range. For cationic complexes, Fe−PAH binding energies were found to be lower by 0.3 eV at the B3LYP/Lanl2dz level than at the MPW1PW91/6-31+G(d,p) level. As discussed by the authors, one has to be careful using thermochemical data obtained at a low level of theory such as B3LYP/Lanl2DZ. In particular, triplet spin states may be overstabilized with respect to quintet spin states due to the fact that the ^{5}D state of Fe is overstabilized with respect to its first ^{3}F triplet spin state.[45] Also BSSE (basis set superposition errors) are expected to occur, but they are expected to be similar in all the complexes studied in this paper. Taking these facts into consideration, the absolute values for binding energies presented in this paper should not be regarded with an accuracy better than 0.3 eV.

III. Results

A. Photodissociation Pathways. As mentionned in section II.A, the dissociation pathways of $[CpFeC_{24}H_{12}]^+$ and $[Cp^*FeC_{24}H_{12}]^+$ were studied in the PIRENEA setup by increasing their internal energy either by the absorption of UV−visible photons or by SORI-CID with He atoms. The photodissociation experiments were performed using the continuous UV−visible irradiation emitted in the 200−800 nm range by a Xenon arc lamp. SORI-CID experiments were performed with helium gas at a pressure of $\sim 5 \times 10^{-7}$ mbar.

In the case of $[CpFeC_{24}H_{12}]^+$, the $CpFe^+$ and Fe^+ fragments were observed under UV−visible irradiation as well as SORI-CID conditions. The mass spectrum of mass-selected $[CpFeC_{24}H_{12}]^+$ recorded after 300 ms irradiation is reported in Figure 2. The following dissociation sequence was identified by selective ejection of the intermediate complex $CpFe^+$:

$$[CpFeC_{24}H_{12}]^+ \rightarrow CpFe^+ + C_{24}H_{12} \rightarrow Cp + Fe^+ + C_{24}H_{12}$$

This sequence is consistent with the relative ionization potentials (IPs) and binding energies (BDEs): the IP of FeCp was found to be lower than that of $C_{24}H_{12}$ (5.5 vs 7.0 eV at the MPW1PW91/6-31+G(d,p) level of theory), implying that the formation of $[CpFe^+ + C_{24}H_{12}]$ is more thermodynamically favorable than that of $[CpFe + C_{24}H_{12}^+]$, which is not observed. In addition, the Fe^+−Cp bond (within 3.3−3.8 eV)[71] is stronger than the $CpFe^+$−$C_{24}H_{12}$ bond estimated at 2.3 ± 0.3 eV at the B3LYP/Lanl2DZ level of theory (cf. section III.C).

In the case of $[Cp^*FeC_{24}H_{12}]^+$, the $C_{10}H_{13}^+$, $[FeC_{10}H_{13}]^+$, $[FeC_{10}H_{15}]^+$, and $C_{24}H_{12}^+$ photofragments were observed under continuous visible irradiation. The mass spectrum of mass-selected $[Cp^*FeC_{24}H_{12}]^+$ recorded after 700 ms irradiation is reported in Figure 3. The two following photodissociation channels were identified:

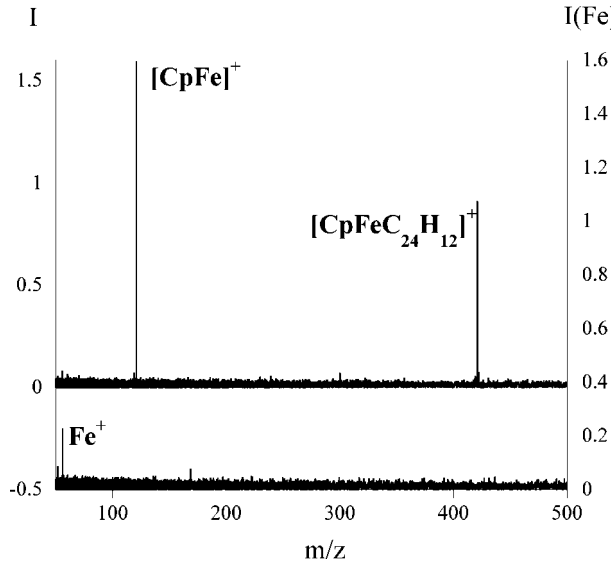

Figure 2. Mass spectrum recorded after 300 ms irradiation of mass-selected $[CpFeC_{24}H_{12}]^+$ in the PIRENEA setup. Irradiation was performed using a Xe arc lamp emitting in the 200−800 nm range.

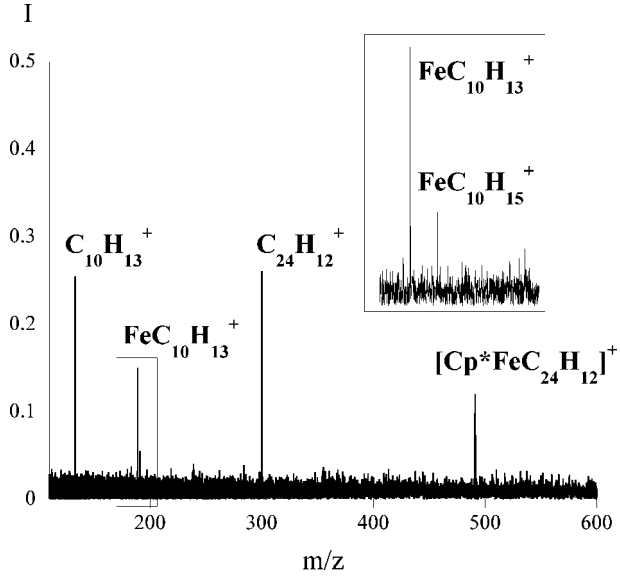

Figure 3. Mass spectrum recorded after 700 ms irradiation of mass-selected $[Cp^*FeC_{24}H_{12}]^+$ in the PIRENEA setup. Irradiation was performed using a Xe arc lamp emitting in the 200−800 nm range.

Channel 1

$$[Cp^*FeC_{24}H_{12}]^+ \rightarrow [C_{10}H_{15}Fe]^+ + C_{24}H_{12} \rightarrow [C_{10}H_{13}Fe]^+ + [2H] + C_{24}H_{12} \rightarrow C_{10}H_{13}{}^+ + Fe + [2H] + C_{24}H_{12}$$

Channel 2

$$[Cp^*FeC_{24}H_{12}]^+ \rightarrow [10C, 15H, Fe] + C_{24}H_{12}{}^+$$

Channels 1 and 2 were found to represent ~60 and 40% of the photodissociation yield, respectively. In SORI-CID experiments, additional fragments were observed, i.e., $C_{24}H_{13}^+$ and $[FeC_{24}H_{13}]^+$ as can be seen in Figure 4. These species were also observed in the IRMPD experiments at FELIX. Additional

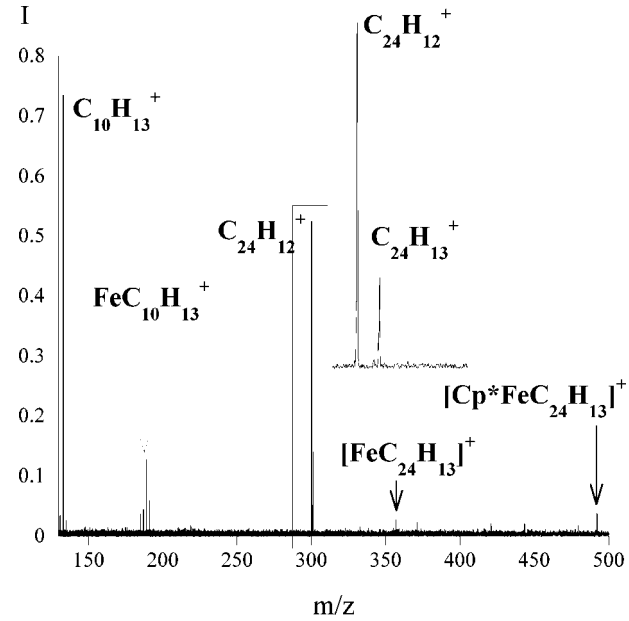

Figure 4. SORI-CID spectrum of mass-selected $[Cp^*FeC_{24}H_{12}]^+$ using a pulse of helium gas at a pressure of 5×10^{-7} mbar.

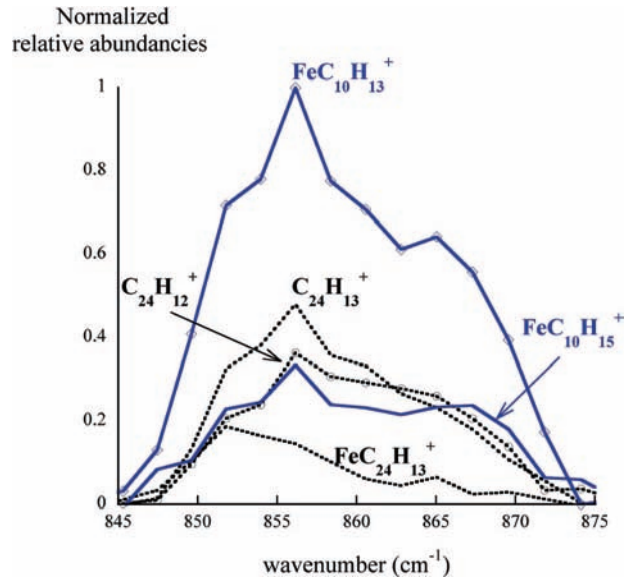

Figure 5. Relative abundancies of the various photofragments observed at FELIX for $[Cp^*FeC_{24}H_{12}]^+$ under irradiation at maximum photodissociation yield: blue solid lines, photofragments from channel 1; dashed lines, photofragments from channel 2.

photodissociation experiments performed on mass-selected $C_{24}H_{13}^+$ show that it easily loses a hydrogen atom.[74] This suggests the following sequence, starting by a hydrogen atom transfer from the Cp* ligand to $C_{24}H_{12}$ coordinated on Fe^+, for channel 2:

$$[Cp^*FeC_{24}H_{12}]^+ \rightarrow [C_{10}H_{14}FeC_{24}H_{13}]^+ \rightarrow C_{10}H_{14} + [FeC_{24}H_{13}]^+ \rightarrow C_{10}H_{14} + Fe + C_{24}H_{13}^+ \rightarrow C_{10}H_{14} + Fe + C_{24}H_{12}^+ + H$$

The full sequence can only be observed under the progressive heating conditions of IRMPD or SORI-CID that allow for a gradual deposit of internal energy into ions inducing widespread fragmentation,[75] whereas some transient species are quickly dissociated under UV−visible irradiation. Both channels 1 and 2 were observed at FELIX under irradiation of $[Cp^*FeC_{24}H_{12}]^+$ at 856 cm^{-1}, where the photodissociation yield is maximum (cf. Figure 5), giving the same branching ratio as under UV−visible irradiation conditions. This supports the scenario of statistical dissociation following IVR and strongly suggests the presence of two types of isomers whose lowest energy fragmentation channels would be respectively 1 and 2.

B. Experimental IRMPD Spectra. The recorded IRMPD spectra of $[CpFeC_{24}H_{12}]^+$ and $[Cp^*FeC_{24}H_{12}]^+$ are shown in Figure 6, which displays the fragmentation yield $P_{frag.}$ as a function of wavenumber. The main feature in the spectra of the two complexes is a band of high intensity at $\sim$ 855 cm^{-1}. The shape of this band is different in the two complexes. It is narrow for $[Cp^*FeC_{24}H_{12}]^+$, whereas it appears broad and structured for $[CpFeC_{24}H_{12}]^+$. The details of this latter band are reported in Figure 6. Secondary maxima are observed at 842, 864, and 879 cm^{-1}. A weak band ($P_{frag.} = 9\%$) also appears at 792 cm^{-1}. At higher energies bands were observed only for $[Cp^*FeC_{24}H_{12}]^+$ with a major feature at 1377 cm^{-1} ($P_{frag.} = 27\%$) and a minor feature ($P_{frag.} = 4\%$) at 1299 cm^{-1}.

The most intense band in both spectra corresponds to the resonance of the C−H out-of-plane bending modes of the aromatic hydrogens (γ_{CH}). In the $[Cp^*FeC_{24}H_{12}]^+$ complex, the only aromatic hydrogens are the ones on the coronene ligand, whereas, in the $[CpFeC_{24}H_{12}]^+$ complex, 5 aromatic hydrogens out of 17 are on the Cp ligand. The weak 1377 and 1299 cm^{-1} bands in the spectrum of $[Cp^*FeC_{24}H_{12}]^+$ are likely to be assigned to the C−H deformation modes of the methyl group and/or a combination of C−H in-plane bending (δ_{CH}) and CC stretching (ν_{CC}) modes within the coronene ligand.

The IRMPD spectra of the complexes are more similar to the absorption spectrum of neutral coronene[7,19,25] than to the absorption and IRMPD spectra of the coronene cation:[5,6,11,19,25] the spectra of the cation are dominated by bands at approximately 1327 and 1533 cm^{-1}, whereas, for neutral coronene, only weak bands are observed in the 1000−1600 cm^{-1} region. These observations are in line with the conclusions drawn by Simon and Joblin[45] on the effects of the coordination of Fe on the theoretical IR spectrum of $C_{24}H_{12}^+$. The most striking effect of this coordination is that the relative intensities of the bands in the 1000−1600 cm^{-1} region vs the one of the γ_{CH} band are strongly decreased. This is also in line with the IRMPD spectra of FeY^+ and FeY_2^+ with Y = C_6H_6, $C_{10}H_8$, and $C_{13}H_{10}$ obtained by Szczepanski et al.[50] using the same experimental setup at FELIX. We also note that, for FeY_2^+ complexes, the most intense γ_{CH} band is split into two bands.

C. Calculated Structures and IR Absorption Spectra. The optimized geometries of the lowest energy structures of $[CpFeC_{24}H_{12}]^+$ and $[Cp^*FeC_{24}H_{12}]^+$ are reported in Figure 7 and Figure 8, respectively. Geometry optimizations were performed without symmetry constraints. Derived thermochemistry data are reported in Table 1.

The ground states for $[CpFeC_{24}H_{12}]^+$ and $[Cp^*FeC_{24}H_{12}]^+$ were found to be in a quintet spin state with the CpFe and Cp*Fe unit coordinated to an outer ring of coronene. For the $[Cp^*FeC_{24}H_{12}]^+$ complexes, only Out isomers were found as minima. Their geometries are similar to those optimized for the $[CpFeC_{24}H_{12}]^+$ complexes. The fact that no In isomers were found can be qualitatively understood as the steric hindrance due to the methyl group of the Cp* ligand can prevent it from sufficiently approaching the iron atom and binding efficiently.

The $XFe^+-C_{24}H_{12}$ binding energies were calculated to be 2.35 and 1.93 eV for X = Cp and X = Cp* respectively (cf. Table 1). These values are consistently lower than the

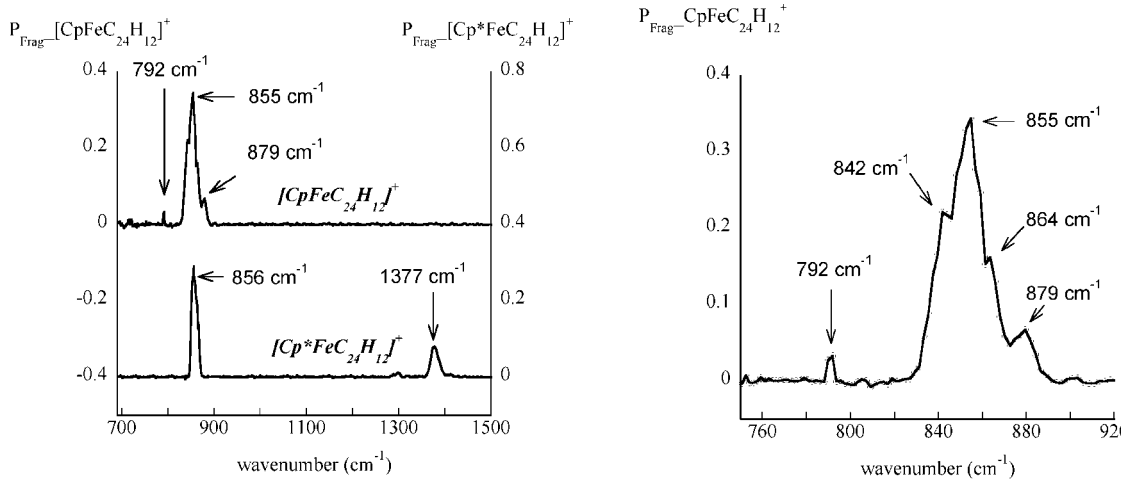

Figure 6. Left: Experimental IRMPD spectra of mass-selected $[CpFeC_{24}H_{12}]^+$ (top) and $[Cp^*FeC_{24}H_{12}]^+$ (bottom). Right: Zoom on the features in the IRMPD spectrum of $[CpFeC_{24}H_{12}]^+$ located between 750 and 920 cm^{-1}.

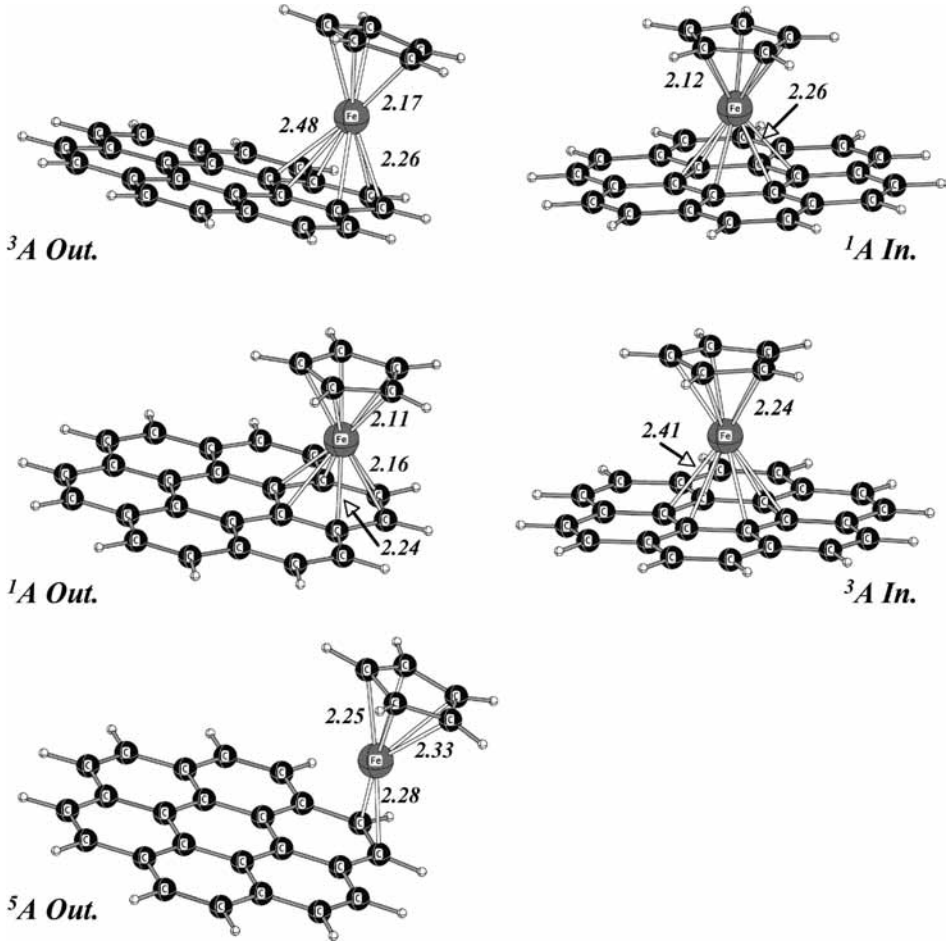

Figure 7. Optimized geometries and electronic states of the lowest energy isomers of $[CpFeC_{24}H_{12}]^+$ at the B3LYP/Lanl2DZ level of theory. The carbon−iron bond lengths are expressed in angstroms.

$Fe^+-C_{24}H_{12}$ binding energy found for the model complex $FeC_{24}H_{12}^+$, estimated at 2.87 eV at the same level of theory.[45] In the $[XFeC_{24}H_{12}]^+$ complex, the positive charge is delocalized on the XFe bond, decreasing the electrostatic interaction between iron and coronene. Besides, additional electron−electron repulsion between the X ligand and coronene can contribute to the lowering of the iron−coronene bond strength. These factors could account for the decrease of 0.5 eV of the iron−coronene binding energy between $FeC_{24}H_{12}^+$ and $[CpFeC_{24}H_{12}]^+$. In Cp*, the methyl groups cause significant steric hindrance. This could explain the reduction of the iron-coronene binding energy by an additional 0.4 eV.

In the ^{5}A Out ground state, iron has an η^2 edge coordination with the Fe atom centered above an outer C−C bond, the iron−carbon distance being 2.28 and 2.29 Å for $[CpFeC_{24}H_{12}]^+$ and $[Cp^*FeC_{24}H_{12}]^+$, respectively. This coordination mode is not common for a binding mode in transition metal−π systems. Interestingly, a similar η^2 edge coordination was found for the $FeC_{24}H_{12}$ neutral complex[45] and for Cu^+−corannulene complexes.[76] Such a coordination mode is expected to optimize the

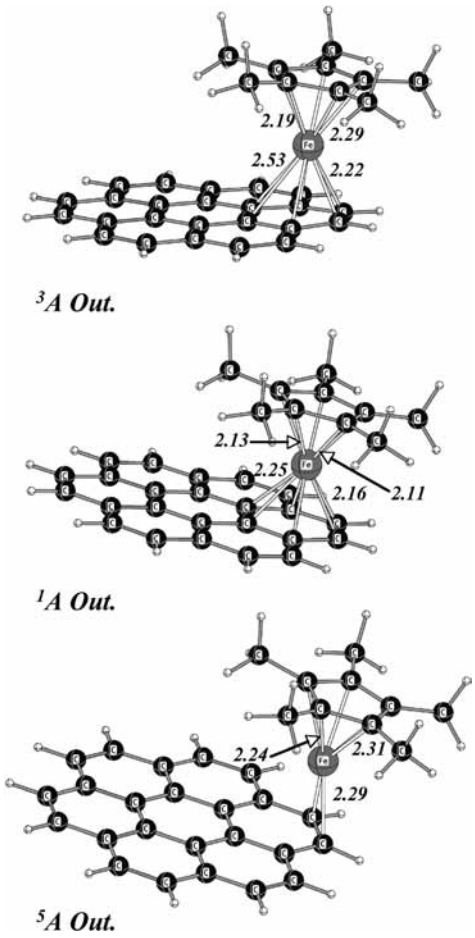

Figure 8. Optimized geometries and electronic states of the lowest energy isomers of $[Cp^*FeC_{24}H_{12}]^+$ at the B3LYP/Lanl2DZ level of theory. The carbon−iron bond lengths are expressed in angstroms.

TABLE 1: Relative Enthalpies at 0 K of the $[XFeC_{24}H_{12}]^+$ (X = Cp, Cp*) Complexes with Respect to the Asymptotes Calculated at the B3LYP/Lanl2DZ Level of Theory (Results Expressed in Electronvolts)

species	isomer	electronic state	ΔH (0 K) (eV)
$CpFe^+ + C_{24}H_{12}$		$^5A + {}^1A_g$	0.0
$[CpFeC_{24}H_{12}]^+$	In	^1A	−1.58
	In	^3A	−1.78
	Out	^3A	−2.01
	Out	^1A	−2.02
	Out	^5A	−2.35
$Cp^*Fe^+ + C_{24}H_{12}$		$^5A + {}^1A_g$	0.0
$[Cp^*FeC_{24}H_{12}]^+$	Out	^3A	−1.78
	Out	^1A	−1.85
	Out	^5A	−1.93

positive overlap between the molecular orbitals responsible for the efficiency of the organometallic bond.[76] The calculated iron−carbon bond length is consistent with the iron−carbon bond length that we calculated at the same level of theory for $FeC_{24}H_{12}^+$ (2.26 Å). A larger value was found for the $FeC_{24}H_{12}$ neutral complex (2.37 Å).

The most common η^6 edge coordination mode was found for the singlet and triplet spin-state isomers (cf. Figures 7 and 8). For the Out isomers, iron is located closer to the external carbon atoms. The ^1A and ^3A Out isomers are found to be very close in energy, especially in the case of $[CpFeC_{24}H_{12}]^+$ (cf. Table 1), with values of 0.33/0.34 eV above the ^5A Out ground state for these species and 0.08/0.15 eV above in the case of $[Cp^*FeC_{24}H_{12}]^+$. The ^3A and ^1A In isomers of $[CpFeC_{24}H_{12}]^+$ are respectively located 0.57 and 0.77 eV above the ground state. Interestingly, $[CpFeC_{24}H_{12}]^+$ complexes were synthetized in the liquid phase via ligand exchange reactions between ferrocene and coronen, and ^1H NMR spectroscopic studies showed that these stable 18-electron complexes present an Out structure.[77] These experiments were completed with electronic structure calculations using the extended Hückel method. In these calculations, the In isomer was found to be less stable than the Out isomer by 0.2 eV and our DFT results are in line with these qualitative results. In addition, the position of the CpFe unit on an outer ring is likely to remain static since according to these extended Hückel calculations, the isomerization from an Out structure to an In structure would have to overcome an energy barrier of 1.5 eV.[77]

The calculated IR spectra of the lowest energy structures for $[CpFeC_{24}H_{12}]^+$ and $[Cp^*FeC_{24}H_{12}]^+$ are reported in Figure 9. In these spectra, the wavenumbers are derived from the calculated frequencies scaled by a factor of 0.929. This scaling factor was adjusted on the neutral coronene spectrum so that the calculated position for the γ_{CH} band matches the experimental position of the γ_{CH} band measured in a neon matrix at 4 K.[7] The calculated discrete spectrum was convoluted by a Lorentzian line profile with a fwhm = 20 cm^{-1} determined using the experimental band located at 1377 cm^{-1} in the IRMPD spectrum of $[Cp^*FeC_{24}H_{12}]^+$. The band positions and their relative intensities with respect to the γ_{CH} band are reported in Table 2 and Table 3 for the calculated lowest energy isomers of $[CpFeC_{24}H_{12}]^+$ and $[Cp^*FeC_{24}H_{12}]^+$, respectively. For all isomers of both species, the γ_{CH} is the most intense band (Figure 9). Its position is the same within 2 cm^{-1} for all the Out isomers. For the ^3A and ^1A In isomers of $[CpFeC_{24}H_{12}]^+$, it is blue-shifted by 7 and 10 cm^{-1}, respectively, compared to the position of the ^5A Out ground state (863 cm^{-1}). This band is assigned to a mixture of CCH and CCC out-of-plane vibrations of $C_{24}H_{12}$ (hence referred to as ϵ and τ; cf. Table 2). Interestingly, the position of the γ_{CH} band in the Out isomers of $[CpFeC_{24}H_{12}]^+$ and $[Cp^*FeC_{24}H_{12}]^+$ (∼862 cm^{-1}) is very similar to the one calculated for the ground state of $[FeC_{24}H_{12}]^+$ (863 cm^{-1}), and it is red-shifted with respect to the position of the γ_{CH} band calculated for $C_{24}H_{12}^+$ (868 cm^{-1}) at the same level of theory.

For the isomers of $[CpFeC_{24}H_{12}]^+$, a band due to the CCH out-of-plane vibrations of the hydrogens of the Cp ligand (ϵ_{Cp}) also appears at lower energy (748−779 cm^{-1}). This band is particularly intense in the spectrum of the ^5A Out ground state (750 cm^{-1}, $I_{norm} = 0.81$). In the case of the Out isomers, the coupling between this mode and the CCC and CCH out-of-plane vibrations of $C_{24}H_{12}$ leads to the occurrence of an additional band ($\epsilon_{Cp} + (\epsilon + \tau)_{cor}$) slightly red-shifted with respect to the ϵ_{Cp} band (4−8 cm^{-1}). The ($\epsilon_{Cp} + (\epsilon + \tau)_{cor}$) band appears even more intense than the ϵ_{Cp} band in the case of the ^1A Out isomer ($I_{norm} = 0.33$ vs 0.11). In $[Cp^*FeC_{24}H_{12}]^+$, the absence of aromatic hydrogens in the Cp* ligand leads to a simpler spectrum in the γ_{CH} region and a richer structural pattern in the 1200−1600 cm^{-1} range due to the presence of methyl groups in Cp* (cf. Figure 9 and Table 3). In the latter region, two groups of modes are identified. The ones at around 1350 cm^{-1} are specific to the Cp* ligand, whereas modes at around 1420 cm^{-1} involve their coupling with the modes of coronene (cf. Table 3). By comparison with the spectra of the $[CpFeC_{24}H_{12}]^+$ complexes, we can conclude that this coupling enhances the band intensities in this spectral range.

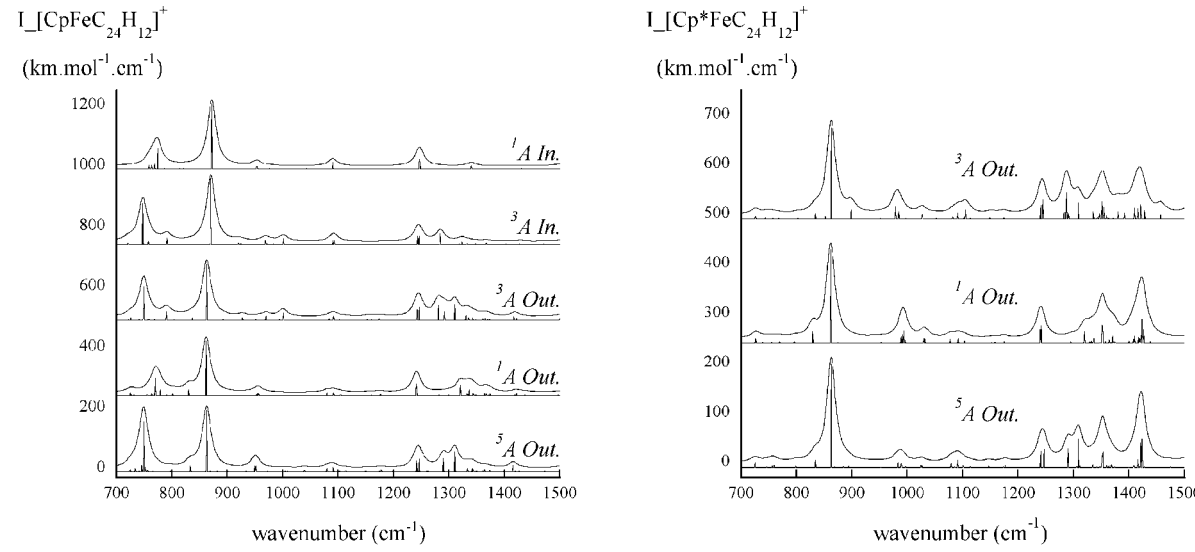

Figure 9. Calculated infrared spectra of the lowest energy isomers of $[CpFeC_{24}H_{12}]^+$ (left) and $[Cp^*FeC_{24}H_{12}]^+$ (right) at the B3LYP/lanl2DZ level of theory. Wavenumbers are derived from the calculated harmonic frequencies scaled by a factor of 0.929. The calculated discrete spectra (sticks) have been convoluted by a Lorentzian profile with a fwhm of 20 cm^{-1}.

TABLE 2: Positions and Relative Intensities (in Parentheses) of the IR Bands Located in the 700−1600 cm^{-1} Range Calculated at 0 K for the Lowest Energy Isomers of $[CpFeC_{24}H_{12}]^+$[a]

	$\nu(I_{norm})$ (cm^{-1})				
Mode	^{5}A Out	^{1}A Out	^{3}A Out	^{3}A In	^{1}A In
$\epsilon_{Cp} + (\epsilon + \tau)_{cor}$	746 (0.11)	771 (0.33)			
ϵ_{Cp}	750 (0.81)	779 (0.11)	750 (0.60)	748 (0.62)	775 (0.32)
$\epsilon_{Cp} + (\alpha + \beta)_{cor}$	752 (0.06)				
$\epsilon_{Cp} + \alpha_{cor}$			790 (0.15)		
$(\epsilon + \tau)_{cor} + \epsilon_{Cp}$	833 (0.09)	831 (0.10)	837 (0.04)		
$(\epsilon + \tau)_{cor}$	863 (1.0)	862 (1.0)	863 (1.0)	870 (1.0)	873 (1.0)
$(R + \beta)_{Cp}$		953 (0.02)			
$(R + \beta)_{Cp}$	951 (0.09)	955 (0.05)	970 (0.06)	969 (0.06)	953 (0.03)
$(R + \beta)_{Cp}$	952 (0.09)	957 (0.04)	999 (0.13)	1002 (0.09)	954 (0.03)
$(\alpha + \beta)_{cor}$	1080 (0.04)			1090 (0.06)	
$(\alpha + \beta)_{cor.}$	1092 (0.07)	1093 (0.05)	1093 (0.06)	1094 (0.06)	1090 (0.09)
$(R + \beta)_{cor}$	1242 (0.17)	1241 (0.17)	1244 (0.18)	1244 (0.12)	1247 (0.14)
$(R + \beta)_{cor}$	1247 (0.20)	1242 (0.21)	1247 (0.23)	1247 (0.13)	1248 (0.14)
$(R + \beta)_{cor}$			1282 (0.27)		
$(R + \beta)_{cor}$	1290 (0.21)		1292 (0.14)	1285 (0.16)	
$(R + \beta)_{cor}$	1311 (0.31)	1321 (0.19)	1312 (0.27)	1324 (0.05)	
$(R + \beta)_{cor}$	1335 (0.01)	1339 (0.11)	1331 (0.08)		
$(R + \beta)_{cor}$	1344 (0.04)		1337 (0.05)		1342 (0.05)
$(R + \beta)_{cor}$	1351 (0.01)		1344 (0.04)		
$(R + \beta)_{cor}$	1374 (0.01)				
$(R + \beta)_{cor}$	1416 (0.10)		1418 (0.06)		
$(R + \beta)_{cor}$	1416 (0.03)	1534 (0.08)			
$(R + \beta)_{cor}$	1541 (0.16)	1543 (0.02)	1541 (0.22)	1536 (0.20)	1534 (0.40)
$(R + \beta)_{cor}$	1541 (0.16)	1548 (0.05)	1543 (0.14)	1541 (0.18)	

[a] The reported wavenumbers are derived from the calculated harmonic frequencies obtained at the B3LYP/Lanl2DZ level of theory scaled by a factor of 0.929 (see text). Only bands with an intensity ratio superior to 1% with respect to the most intense band of the spectrum are reported. Notations used are as follows:[47] α and β are CCC and CCH in-plane bending modes, τ and ϵ are CCC and CCH out-of-plane vibrations, and R is the CC stretching mode. Subscripts cor and Cp refer to the coronene and Cp ligands, respectively.

D. IRMPD Experimental Spectra vs Calculated IR Spectra. The comparison between the two IRMPD spectra shows two main differences: (i) a broad and structured γ_{CH} band with an additional low-intensity band at 792 cm^{-1} in the case of $[CpFeC_{24}H_{12}]^+$ and (ii) the presence of two bands at 1377 and 1299 cm^{-1} in the case of $[Cp^*FeC_{24}H_{12}]^+$, whereas no band is observed in the 1200−1600 cm^{-1} region for $[CpFeC_{24}H_{12}]^+$. The first difference can be accounted for by the coupling between the γ_{CH} modes of the two types of aromatic hydrogens as discussed in section III.C, and this coupling cannot be properly described by the calculations. Item (ii) is related to the nonlinearity of the IRMPD process, as it was concluded for $C_{24}H_{12}^+$.[11] In the particular case of large systems such as PAHs, IVR is very fast and dissociation occurs statistically when the internal energy is high enough, leading to a threshold effect due to the large heat capacity of the molecule. This implies that only the most intense bands are expected to be observed. Thus, the calculated band intensities of $[Cp^*FeC_{24}H_{12}]^+$ in the 1200−1600 cm^{-1} range being higher on average than that of $[CpFeC_{24}H_{12}]^+$ is consistent with the IRMPD spectra. Given these processes and the presence of three low-energy isomers of different spin states with similar geometric structures and

TABLE 3: Positions and Relative Intensities (in Parentheses) of the IR Bands Located in the 700−1600 cm^{-1} Range Calculated at 0 K for the Lowest Energy Isomers of [Cp*FeC$_{24}$H$_{12}$]$^{+a}$

Mode	ν (I $_{Norm.}$) (cm^{-1})		
	^{5}A Out	^{1}A Out	^{3}A Out
$(\epsilon_{oo\phi} + \tau)_{cor}$	834 (0.07)	829 (0.13)	826 (0.06)
$(\epsilon_{in\phi} + \tau)_{cor}$	863 (1.0)	861 (1.0)	862 (1.0)
$\rho_{CH_3} + R_{C-C(Cp*)}$			898 (0.11)
ρ_{CH_3}	983 (0.05)	988 (0.07)	976 (0.08)/978 (0.14)
ρ_{CH_3}	990 (0.04)	993 (0.13)/982 (0.09)	
ρ_{CH_3}	1025 (0.02)		1026 (0.06)
β_{cor}	1080 (0.04)		1091 (0.07)
β_{cor}	1092 (0.07)		1105 (0.10)
$(R + \beta)_{cor}$	1241 (0.16)	1239 (0.15)	1239 (0.16)
$(R + \beta_{cor}$	1247 (0.17)	1241 (0.19)	1244 (0.21)
$(R + \beta)_{cor}$	1290 (0.18)		1290 (0.06) /1286 (0.30)/1282 (0.08)
$(R + \beta)_{cor} + R_{C-CH_3} + \nu_{CH_3}$	1308 (0.27)	1318 (0.12)	1308 (0.18)
$(R + \beta)_{cor}$			1334 (0.09)
$\nu_{CH_3} + R_{C-CH_3}$	1352 (0.08)		1345 (0.06)
$\nu_{CH_3} + R_{C-CH_3}$	1352 (0.12)	1350 (0.19)	1350 (0.20)
$\nu_{CH_3} + R_{C-CH_3}$	1354 (0.15)	1352 (0.16)	1354 (0.16)
$\nu_{CH_3} + R_{C-C(Cp*)}$		1370 (0.08)	1380 (0.09)
$\delta_{CH_3} + R_{C-C(Cp*)}$			1391 (0.07)
δ_{CH_3}		1409 (0.08)	1409 (0.12)
$\delta_{CH_3} + R_{C-CH_3} + \beta_{cor}$		1417 (0.06)	1415 (0.12)
$\delta_{CH_3} + R_{C-CH_3} + \beta_{cor}$	1421 (0.22)	1421 (0.09)	1421 (0.16)
$\delta_{CH_3} + R_{C-CH_3} + \beta_{cor}$	1423 (0.10)	1423 (0.26)	1421 (0.08)
$\delta_{CH_3} + R_{C-CH_3} + \beta_{cor}$	1425 (0.27)	1425 (0.14)	1427 (0.10)
$(R + \beta)_{cor}$		1531 (0.08)	1538 (0.16)
$(R + \beta)_{cor}$	1540 (0.26)	1542 (0.14)	1542 (0.12)

[a] The reported wavenumbers are derived from the calculated harmonic frequencies obtained at the B3LYP/Lanl2DZ level of theory scaled by a factor of 0.929 (see text). Only bands with an intensity ratio superior to 1% with respect to the most intense band of the spectrum are reported. Notations used are as follows:[47] α and β are CCC and CCH in-plane bending modes, τ and ϵ are CCC and CCH out-of-plane vibrations, and R is the CC stretching mode. Subscripts cor and Cp refer to the coronene and Cp ligands, respectively.

IR absorption spectra, the assignment to a specific spin state is delicate. Still, we can get some insights into this question.

In the case of [CpFeC$_{24}$H$_{12}$]$^+$, the ^{1}A Out isomer seems to be favored. Indeed, as mentionned above, the characteristics of the IRMPD spectrum of [CpFeC$_{24}$H$_{12}$]$^+$ in the 700−900 cm^{-1} region can be understood by the presence of two types of aromatic hydrogens that are coupled. This leads one to propose the Out structures, which are also the most stable ones in the calculations (Table 1), as the ones formed in the experiment. By comparing the IRMPD spectrum and the calculated IR absorption spectra (Figures 6 and 9, Table 2), the band at 792 cm^{-1} can be assigned to the γ_{CH} mode of the aromatic hydrogens of Cp probably combined with the CCH and CCC out-of-plane vibrations of C$_{24}$H$_{12}$. Among the calculated IR spectra, the one of the ^{1}A Out isomer appears to be the most consistent with this feature of the experimental spectrum with a calculated (ϵ_{Cp} + $(\epsilon + \tau)_{cor}$) band located at 771 cm^{-1} and a "satellite" weaker ϵ_{Cp} band appearing at 779 cm^{-1} (Table 2). The two other Out isomers present a strong band at 750 cm^{-1}, further from the experimental value of 792 cm^{-1}, which would have appeared more clearly in the IRMPD spectrum. Given the accuracy of the DFT calculations, it is not excluded that the ^{1}A Out isomer, located 0.33 eV above the ^{5}A Out isomers at the B3LYP/Lanl2DZ level of theory (Table 1), cannot be found as the ground state at a higher level of theory. The ^{1}A In isomer was found to be higher in energy than the ^{1}A Out isomer by ~0.4 eV at the B3LYP/Lanl2DZ level of theory (Table 1). The comparison between calculated and experimental spectra does not allow one to rule out its presence in minor abundance. As an example, the theoretical IR spectrum taking into account the presence of these two isomers in a 2:1 ratio is reported in Figure 10 below the experimental IRMPD spectrum of [CpFeC$_{24}$H$_{12}$]$^+$.

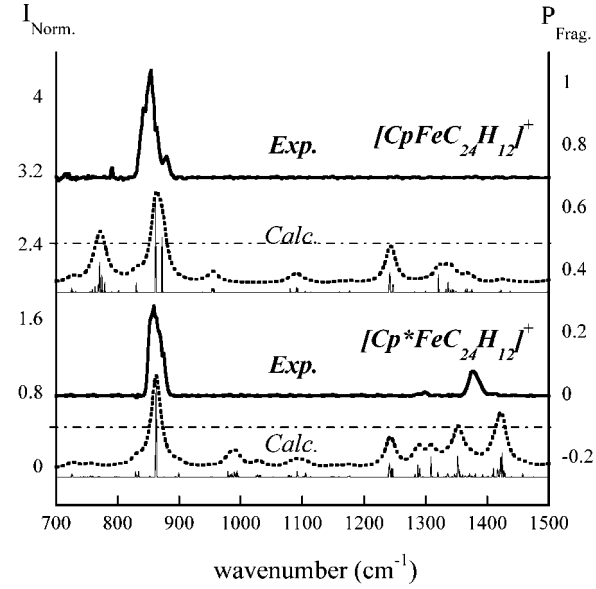

Figure 10. Normalized intensities of the sum of the calculated IR spectra for (i) the ^{1}A Out and ^{1}A In isomers of [CpFeC$_{24}$H$_{12}$]$^+$ in a 2:1 ratio (top) and (ii) the ^{5}A, ^{1}A, and ^{3}A Out isomers of [Cp*FeC$_{24}$H$_{12}$]$^+$ in a 1:1:1 ratio (bottom). The dashed horizontal lines represent the threshold value for I_{norm} under which the IR band is not observed. Experimental IRMPD spectra (solid lines) are also reported.

This shows that the presence of the ^{1}A In isomer may also contribute to the broadening of the γ_{CH} band.

In the case of [Cp*FeC$_{24}$H$_{12}$]$^+$, the comparison between the IRMPD spectrum and the IR absorption spectra does not allow assignment of a specific isomer. It is actually likely that the three ^{5}A, ^{1}A, and ^{3}A Out isomers are observed simultaneously.

The spectrum of the normalized IR intensity taking into account these three isomers in a 1:1:1 ratio is reported in Figure 10 below the IRMPD spectrum. The presence of these three isomers would be consistent with the two observed dissociation pathways and branching ratios detailed in section IIIA. We can tentatively propose that channel 2 would occur for the ^{5}A Out isomer that appears to be more flexible (given the edge position of the FeCp* unit) and thus more favorable to hydrogen transfers, whereas channel 1 would be observed for the ^{1}A and ^{3}A Out isomers. Given that the three isomers were found within 0.2 eV at the B3LYP/Lanl2DZ level of calculation (cf. Table 1), which is below the uncertainty of the method, it is reasonable to assume that they are present in equivalent proportion, following a thermal distribution. Therefore, one would expect a 66% ratio for channel 1 and 33% ratio for channel 1, which is consistent with the branching ratios measured experimentally ($\sim$ 60% for channel 1 and $\sim$ 40% for channel 2; cf. section III.A).

Figure 10 summarizes our results. From the study of the $[CpFeC_{24}H_{12}]^+$ complexes, we can derive a minimum I_{norm} value of $\sim$0.4 below which the IRMPD process is not efficient. Applying a similar threshold to the average calculated spectrum of the $[Cp^*FeC_{24}H_{12}]^+$ isomers allows an explanation of the presence of bands in the 1200−1600 cm^{-1} range. Still, the measured position at 1377 cm^{-1} is significantly shifted from the calculated band at 1423 cm^{-1}. This cannot be explained by temperature effects only and gives more evidence for strong mode couplings in these $[XFeC_{24}H_{12}]^+$ species.

E. Astrophysical Implications. We discuss the relevance of our combined experimental and theoretical approaches to better characterize the energetics and IR spectroscopy of iron complexes with large PAHs, these systems being of interest for astrochemistry. Simon and Joblin put forward that the main effect of the coordination of iron on cationic PAHs is the significant decrease of the relative intensities in the 1000−1600 cm^{-1} region vs the 600−1000 cm^{-1} region.[45] This was confirmed experimentally for $FeC_6H_6^+$ and $FeC_{10}H_8^+$,[50] and this study is an experimental verification of this trend using the $[XFeC_{24}H_{12}]^+$ (X = Cp, Cp*) species as model complexes. Besides, the calculated IR spectra of $[XFeC_{24}H_{12}]^+$ (X = Cp, Cp*) confirm that the red (respectively blue) shift of the γ_{CH} band of $C_{24}H_{12}^+$ (respectively $C_{24}H_{12}$) upon coordination of iron ($\sim$5 cm^{-1}) is too small to be used as a diagnosis for the presence of iron−PAH species in the ISM. The calculated values of the $XFe^+-C_{24}H_{12}$ binding energies (2.3 $\pm$ 0.3 eV for X = Cp and 1.9 $\pm$ 0.3 eV for X = Cp*) are in qualitative agreement with the observed dissociation schemes: no loss of hydrogen atom from $C_{24}H_{12}$ is observed, in line with a larger $H-C_{24}H_{11}$ bond energy ($\sim$4.8 eV). These values are of interest for astrochemical models as they allow to calculate the lifetime of these complexes in various interstellar environments, e.g., the competition between formation and photodissociation as was investigated by Rapacioli et al.[78] for PAH clusters. These studies were indeed motivated by the observation that interstellar PAHs are released by evaporation of very small grains (VSGs) under UV irradiation in photodissociation regions (PDRs) where chemistry is governed by UV photons.[34,79] Similarly to pure PAH clusters, mixed Fe−PAH nanograins have to be tested as possible candidates for these VSGs since the photodissociation pathways observed for $[XFeC_{24}H_{12}]^+$ (X = Cp, Cp*) show that large aromatic hydrocarbon units can be released.

IV. Conclusion

This study adds to the growing database on PAH-like species of potential astronomical relevance. It presents the first experimental IRMPD spectra of gas-phase $[XFeC_{24}H_{12}]^+$ (X = Cp, Cp*) complexes recorded at FELIX. This is the first time that such spectra are obtained for organometallic complexes containing a PAH as large as $C_{24}H_{12}$. These results are complemented with calculated IR absorption spectra in the harmonic approximation at the DFT level. The comparison between experiment and theory enables further characterization of the geometry and thermodynamics of these complexes. The isomers in which the XFe unit is coordinated to an outer ring of $C_{24}H_{12}^+$ (Out isomers) were calculated to be the most stable ones. For $[CpFeC_{24}H_{12}]^+$ complexes, the ^{1}A Out isomer appears to be the best candidate to be formed in the experiment but the formation of the ^{1}A In higher energy isomer in minor abundance is also likely. For $[Cp^*FeC_{24}H_{12}]^+$ complexes, a specific spin state cannot be assigned, and it is even probable that the three calculated isomers of similar energy are formed. That would be in qualitative agreement with the observed dissociation patterns. The photodissociation pathways and the observed shifts between calculated and experimental bands are in line with the $CpFe^+-C_{24}H_{12}$ and $H-C_{24}H_{11}^+$ relative binding energies. For the systems under study here, a threshold in the calculated IR intensities below which the IRMPD bands cannot be observed, has been deduced. Strong mode couplings are also evidenced which cannot be described by the current calculations. Overall, the experimental and calculated data presented in this work give support to the conclusions drawn by Simon and Joblin[45] on the change of the $C_{24}H_{12}^+$ spectrum upon coordination of Fe that consists in weakening the bands in the 1000−1600 cm^{-1} region. The observed photodissociation pathways also provide primary support for Fe−PAH complexes as good candidates for astronomical VSGs. The next step is to obtain the IR spectra of multimetal−multiligand $[Fe_x(C_{24}H_{12})_y]^+$ complexes that were recently formed and photoevaporated in the PIRENEA setup.[80]

Acknowledgment. We gratefully acknowledge the support of the Stichting voor Fundamenteel Onderzoek der Materie (FOM) in providing beam time on FELIX. We thank the FELIX staff for their skillfull assistance, in particular Dr. Lex van der Meer and Dr. Britta Redlich for their technical help and logistics support. A.S. and C.J. gratefully acknowledge the European FP6 program for providing the support for travel and subsistence at FELIX. A.S. acknowledges the Groupement Scientifique CALMIP (http://www.calmip.cict.fr) of Université Toulouse III that allowed her to perform DFT calculations on the SOLEIL calculator. Support from the French National Program,"Physique et Chimie du Milieu Interstellaire" is also acknowledged. Finally, we thank the reviewers for their comments that considerably helped to improve the manuscript.

References and Notes

(1) Léger, A.; Puget, J.-L. *Astron. Astrophys.* **1984**, *137*, L5.
(2) Allamandola, L. J.; Tielens, A. G. G. M.; Barker, J. R. *Astrophys. J.* **1985**, *290*, L25.
(3) Cook, D. J.; Schlemmer, S.; Balucani, N.; Wagner, D. R.; Harrison, J. A.; Steiner, B.; Saykally, R. J. *J. Phys. Chem. A* **1998**, *102*, 1465.
(4) Hudgins, D. M.; Sandford, S. A.; Allamandola, L. J. *J. Phys. Chem.* **1994**, *98*, 4243.
(5) Hudgins, D. M.; Allamandola, L. J. *J. Phys. Chem.* **1995**, *99*, 3033.
(6) Hudgins, D. M.; Allamandola, L. J. *J. Phys. Chem.* **1995**, *99*, 8978.
(7) Joblin, C.; D'Hendecourt, L.; Léger, A.; Defourneau, D. *Astron. Astrophys.* **1994**, *281*, 923.
(8) Joblin, C.; Boissel, P.; Léger, A.; D'Hendecourt, L.; Defourneau, D. *Astron. Astrophys.* **1995**, *299*, 835.
(9) Kim, H.-S.; Wagner, D. R.; Saykally, R. J. *Phys. Rev. Lett.* **2001**, *86*, 5691.
(10) Kim, H.-S.; Saykally, R. J. *Astrophys. J., Suppl. Ser.* **2002**, *143*, 455.

(11) Oomens, J.; Sartakov, B. G.; Tielens, A. G. G. M.; Meijer, G.; Helden, G. *Astrophys. J.* **2001**, *560*, L99.
(12) Oomens, J.; Tielens, A. G. G. M.; Sartakov, B. G.; von Helden, G.; Meijer, G. *Astrophys. J.* **2003**, *591*, 968.
(13) Szczepanski, J.; Vala, M. *Astrophys. J.* **1993**, *414*, 646.
(14) Szczepanski, J.; Vala, M. *Nature* **1993**, *363*, 699.
(15) Bauschlicher, C. W., Jr.; Partridge, H.; Langhoff, S. R. *J. Phys. Chem.* **1992**, *96*, 3273.
(16) de Frees, D. J.; Miller, M. D.; Talbi, D.; Pauzat, F.; Ellinger, Y. *Astrophys. J.* **1993**, *408*, 530.
(17) Pauzat, F.; Talbi, D.; Ellinger, Y. *Astron. Astrophys.* **1995**, *293*, 263.
(18) Pauzat, F.; Talbi, D.; Ellinger, Y. *Astron. Astrophys.* **1997**, *319*, 318.
(19) Langhoff, S. R. *J. Phys. Chem.* **1996**, *100*, 2819.
(20) Ellinger, Y.; Pauzat, F.; Lengsfield, B. H. *J. Mol. Struct.* **1999**, *458*, 203.
(21) Pauzat, F.; Ellinger, Y. *Chem. Phys.* **2002**, *280*, 267.
(22) Bauschlicher, C. W., Jr *Astrophys. J.* **2002**, *564*, 782.
(23) Hudgins, D. M.; Bauschlicher, C. W., Jr.; Allamandola, L. J *Astrophys. J.* **2005**, *632*, 316.
(24) Malloci, G.; Joblin, C.; Mulas, G. *Astron. Astrophys.* **2006**, *462*, 627.
(25) Malloci, G.; Joblin, C.; Mulas, G. *Chem. Phys.* **2007**, *332*, 353.
(26) Allamandola, L. J.; Hudgins, D. M.; Sandford, S. A *Astrophys. J.* **1999**, *511*, L115.
(27) Bakes, E. L. O.; Tielens, A. G. G. M. *Astrophys. J.* **1994**, *427*, 822.
(28) Bakes, E. L. O.; Tielens, A. G. G. M.; Bauschlicher, C. W., Jr *Astrophys. J.* **2001**, *556*, 501.
(29) Boulanger, F.; Boissel, P.; Cesarsky, D.; Ryter, C. *Astron. Astrophys.* **1998**, *339*, 194.
(30) Hony, S.; Van Kerckhoven, C.; Peeters, E.; Tielens, A. G. G. M.; Hudgins, D. M.; Allamandola, L. J. *Astron. Astrophys.* **2001**, *370*, 1030.
(31) Pech, C.; Joblin, C.; Boissel, P. *Astron. Astrophys.* **2002**, *388*, 639.
(32) Schutte, W. A.; Tielens, A. G. G. M.; Allamandola, L. J. *Astrophys. J.* **1993**, *415*, 397.
(33) Verstraete, L.; Pech, C.; Moutou, C.; Sellgren, K.; Wright, C. M.; Giard, M.; Léger, A.; Timmermann, R.; Drapatz, S. *Astron. Astrophys.* **2001**, *372*, 381.
(34) Rapacioli, M.; Joblin, J.; Boissel, P. *Astron. Astrophys.* **2005**, *429*, 193.
(35) van Diedenhoven, B.; Peeters, E.; Van Kerckhoven, C.; Hony, S.; Hudgins, D. M.; Allamandola, L. J.; Tielens, A. G. G. M. *Astrophys. J.* **2004**, *611*, 928.
(36) Peeters, E.; Hony, S.; Van Kerckhoven, C.; Tielens, A. G. G. M.; Allamandola, L. J.; Hudgins, D. M.; Bauschlicher, C. W. *Astron. Astrophys.* **2002**, *390*, 1089.
(37) Serra, G.; Chaudret, B.; Saillard, Y.; Le Beuze, A.; Rabaâ, H.; Ristorcelli, I.; Klotz, A. *Astron. Astrophys.* **1992**, *260*, 489.
(38) Chaudret, B.; Le Beuze, A.; Rabaâ, H.; Saillard, Y.; Serra, G. *New J. Chem.* **1991**, *15*, 791.
(39) Ristorcelli, I.; Klotz, A. *Astron. Astrophys.* **1997**, *317*, 962.
(40) Marty, P.; de Parseval, P.; Klotz, A.; Chaudret, B.; Serra, G.; Boissel, P. *Chem. Phys. Lett.* **1996**, *256*, 669.
(41) Marty, P.; de Parseval, P.; Klotz, A.; Serra, G.; Boissel, P. *Astron. Astrophys.* **1996**, *316*, 270.
(42) Cassam-Chenai, P. *Planet. Space Sci.* **2002**, *50*, 871.
(43) Marty, P.; Serra, G.; Chaudret, B.; Ristorcelli, I. *Astron. Astrophys.* **1994**, *282*, 916.
(44) Klotz, A.; Marty, P.; Boissel, P.; Serra, G.; Chaudret, B.; Daudey, J.-P. *Astron. Astrophys.* **1995**, *304*, 520.
(45) Simon, A.; Joblin, C. *J. Phys. Chem. A* **2007**, *111*, 9745.
(46) Elustondo, E.; Dalibart, M.; Deroult, J.; Mascetti, J. *Phys. Chem. Earth Part C-Sol. Terrest. Planet. Science* **1999**, *24*, 583.
(47) Wang, Y.; Szczepanski, J.; Vala, M. *Chem. Phys.* **2007**, *342*, 107.
(48) Oepts, D.; van der Meer, A. F. G.; Amersfoot, P. W. *Infrared Phys. Technol.* **1995**, *36*, 297.
(49) Oomens, J.; Sartakov, B. G.; Meijer, G.; von Helden, G. *Int. J. Mass Spectrom.* **2006**, *254*, 1.
(50) Szczepanski, J.; Wang, H.; Vala, M.; Tielens, A. G. G. M.; Eyler, J. R.; Oomens, J. *Astrophys. J.* **2006**, *646*, 666.
(51) Dunbar, R. C.; Polfer, N. C.; Oomens, J. *J. Am. Chem. Soc.* **2007**, *129*, 14562.
(52) Polfer, N. C.; Oomens, J.; Suhai, S.; Paizs, B. *J. Am. Chem. Soc.* **2007**, *129*, 5887, and references therein.
(53) Wu, R. H.; McMahon, T. B. *J. Am. Chem. Soc.* **2007**, *129*, 11312.
(54) Simon, A.; MacAleese, L.; Maître, P.; Lemaire, J.; McMahon, T. B. *J. Am. Chem. Soc.* **2007**, *129*, 2829, and references therein.
(55) MacAleese, L.; Maître, P. *Mass Spectrom. Rev.* **2007**, *26*, 583, references herein
(56) Pozniak, B. P.; Dunbar, R. C. *J. Am. Chem. Soc.* **1997**, *119*, 10439.
(57) Ayers, T. M.; Westlake, B. C.; Duncan, M. A. *J. Phys. Chem. A* **2004**, *108*, 9805.
(58) Buchanan, J. W.; Reddic, J. E.; Grieves, G. A.; Duncan, M. A. *J. Phys. Chem. A* **1998**, *102*, 6390.
(59) Joblin, C.; Pech, C.; Armengaud, M.; Frabel, P.; Boissel, P. In *a Piece of Interstellar Medium in the Laboratory: The PIRENEA Experiment*; EAS Publications Series, Vol. 4, Proceedings of Infrared and Submillimeter Space Astronomy, June 11–13, 2001; Giard, M.; Bernard, J. P.; Klotz, A. and Ristorcelli, I. Eds.; EDP Sciences, 2002, p. 73.
(60) Valle, J. J.; Eyler, J. R.; Oomens, J.; Moore, D. T.; van der Meer, A. F. G.; von Helden, G.; Meijer, G.; Hendrickson, C. L.; Marshall, A. G.; Blakney, G. T. *Rev. Sci. Instrum.* **2005**, *76*, 023103.
(61) Wang, T. C.; Ricca, T. L.; Marshall, A. G. *Ann. Chem.* **1986**, *58*, 2935.
(62) Guan, S.; Marshall, A. G. *Int. J. Mass Spectrom. Ion Process* **1996**, *5*, Vol. 157–158, p 5.
(63) Black, J. G.; Yablonovitch, E.; Bloembergen, N.; Mukamel, S. *Phys. Rev. Lett.* **1977**, *38*, 1131.
(64) Grant, E. R.; Schulz, P. A.; Sudbo, A. S.; Shen, Y. R.; Lee, Y. T. *Phys. Rev. Lett.* **1978**, *40*, 115.
(65) Heck, A. J. R.; de Koning, L. J.; Pinske, F. A.; Nibbering, N. M. M. *Rapid Commun. Mass Spectrom.* **1991**, *5*, 406.
(66) Gauthier, J. W.; Trautman, T. R.; Jacobson, D. B. *Anal. Chem. Acta* **1991**, *246*, 211.
(67) Stevens, P. J.; Devlin, F. J.; Chablowski, C. F.; Frisch, M. J. *J. Phys. Chem. A* **1994**, *98*, 11623.
(68) Hay, P. J.; Wadt, W. R. *J. Chem. Phys.* **1985**, *82*, 270.
(69) Frisch, M. J.; Trucks, G. W.; Schlegel, H. B.; Scuseria, G. E.; Robb, M. A.; Cheeseman, J. R.; Zakrzewski, V. G.; Montgomery, J. A., Jr.; Stratmann, R. E.; Burant, J. C.; Dapprich, S.; Millam, J. M.; Daniels, A. D.; Kudin, K. N.; Strain, N. C.; Farkas, O.; Tomasi, J.; Barone, V.; Cossi, M.; Cammi, R.; Mennucci, B.; Pomelli, C.; Adamo, C.; Clifford, S.; Ochterski,J.; Petersson, G. A.; Ayala, P. Y.; Cui, Q.; Morokuma, K.; Malick, D. K.; Rabuck, A. D.; Raghavachari, K.; Foresman, J. B.; Cioslowski, J.; Ortiz, J. V.; Stefanov, B. B.; Liu, G.; Liashenko, A.; Piskorz, P.; Komaromi, I. ; Gomperts, R. ; Martin, R. L. ; Fox, D. J. ; Keith, T. ; Al-Laham, M. A. ; Peng, C. Y.; Nanayakkara, A. ; Gonzalez, C. ; Challacombe, M. ; Gill, P. M. W. ; Johnson, B. ; Chen, W. ; Wong, M. W. ; Andres, J. L. ; Gonzalez, C. ; Head-Gordon, M. ; Replogle, E. S. ; Pople, J. A. *Gaussian 03*, Revision A.1; Gaussian, Inc.: Pittsburgh, PA, 2003.
(70) *NIST Atomic Spectra Database*, version 3.1.2;Ralchenko, Y., Jou, F.-C. , Kelleher, D. E., Kramida, A. E., Musgrove, A., Reader, J. , Wiese, W. L., Olsen, K., Eds.; National Institute of Standards and Technology: Gaithersburg, MD, 2007.
(71) Sodupe, M.; Bauschlicher, C. W. *J. Chem. Phys. Lett.* **1993**, *207*, 19.
(72) Adamo, C.; Barone, V. *Chem. Phys. Lett.* **1997**, *274*, 242.
(73) Adamo, C.; Barone, V. *J. Chem. Phys.* **1998**, *108*, 664.
(74) Simon, A.; Joblin, C., Unpublished data.
(75) Guo, X.; Duursma, M. C.; Al- Khalili, A.; Heeren, R. M. A. *Int. J. Mass Spectrom.* **2003**, *225*, 71.
(76) Dunbar, R. C. *J. Phys. Chem. A* **2002**, *106*, 9809.
(77) Schmitt, G.; Keim, W. *J. Organomet. Chem.* **1978**, *152*, 315.
(78) Rapacioli, M.; Calvo, F.; Joblin, C.; Parneix, P.; Toublanc, D.; Spiegelman, F. *Astron. Astrophys.* **2006**, *460*, 519.
(79) Berné, O.; Joblin, C.; Deville, Y.; Smith, J. D.; Rapacioli, M.; Bernard, J. P.; Thomas, J.; Reach, W.; Abergel, A. *Astron. Astrophys.* **2007**, *469*, 575.
(80) Simon, A.; Joblin, C. *Astron. Astrophys.*, submitted for publication.

JP801517Q